

Ensembles of Random SHAPs

Lev V. Utkin and Andrei V. Konstantinov
 Peter the Great St.Petersburg Polytechnic University
 St.Petersburg, Russia
 e-mail: lev.utkin@gmail.com, andrue.konst@gmail.com

Abstract

Ensemble-based modifications of the well-known SHapley Additive exPlanations (SHAP) method for the local explanation of a black-box model are proposed. The modifications aim to simplify SHAP which is computationally expensive when there is a large number of features. The main idea behind the proposed modifications is to approximate SHAP by an ensemble of SHAPs with a smaller number of features. According to the first modification, called ER-SHAP, several features are randomly selected many times from the feature set, and Shapley values for the features are computed by means of “small” SHAPs. The explanation results are averaged to get the final Shapley values. According to the second modification, called ERW-SHAP, several points are generated around the explained instance for diversity purposes, and results of their explanation are combined with weights depending on distances between points and the explained instance. The third modification, called ER-SHAP-RF, uses the random forest for preliminary explanation of instances and determining a feature probability distribution which is applied to selection of features in the ensemble-based procedure of ER-SHAP. Many numerical experiments illustrating the proposed modifications demonstrate their efficiency and properties for local explanation.

Keywords: explanation model, XAI, SHAP, random forest, ensemble model.

1 Introduction

Machine learning models and algorithms have shown an increasing importance and success in many domains. Despite the success, there are obstacles for applying machine learning algorithms especially in areas of risk, for example, in medicine, reliability maintenance, autonomous vehicle systems, security applications. One of the obstacles is that many machine learning models have sophisticated architectures and, therefore, they are viewed as black boxes. As a result, models have the limited interpretability, and a user of the corresponding model cannot understand and explain the predictions and decisions provided by the model. Another obstacle is that a single testing instance has to be explained in many cases, i.e., a user needs to understand only a single prediction, for example, a diagnosis of a patient stated by a model. In order to overcome these obstacles, additional interpretable models should be developed that could help to answer the question, which features of an analyzed instance lead to the black-box survival model prediction. In other words, these models should select the most important features which impact on the black-box model prediction. It should be noted that some models, including linear regression, logistic

regression, decision trees are intrinsically explainable due to their peculiarities. At the same time, most machine learning models, especially, deep learning models are black boxes and cannot be directly explained. Explanation of these models and their predictions motivated developing a lot of methods and models which try to explain predictions of the deep classification and regression algorithms. There are several detailed survey papers providing a deep dive into variety of interpretation methods and models [7, 23, 31, 35, 36, 54, 57, 60], which show an increasing importance of the interpretation methods and a growing interest to them.

Interpretation of the black-model local prediction aims to select features which significantly impact on this prediction, i.e., by using the interpretation model, we try to determine *which features of an analyzed instance lead the obtained black-box model prediction*. There are two groups of the interpretation methods. The first one consists of the so-called local methods. They try to interpret a black-box model locally around a test instance. The second group contains global methods which derive interpretations on the whole dataset or its part. The present paper focuses on the first group of the local interpretation methods though the proposed approach can be simply extended to the global interpretation.

Two very popular post-hoc approaches to interpretation can be selected among many others. The first one is LIME (Local Interpretable Model-Agnostic Explanation) [41], which is based on building an approximating linear model around the instance to be explained. This follows from the intuition that the explanation may be derived locally from many instances generated in the neighborhood of the explained instance with weights defined by their distances from the explained instance. Coefficients of the linear model are interpreted as the feature’s importance. The linear regression for solving the regression problem or logistic regression for solving the classification problem allow us to construct the corresponding linear models. LIME has many advantages. It successfully interprets models dealing with tabular data, text, and images. However, there are some shortcomings of LIME. The first one is that LIME is not robust. This means that it may provide very different explanations for two nearby data points. The definition of neighborhoods is also very vague. Moreover, LIME may provide incorrect explanation when there is a small difference between training and testing data. LIME is also sensitive to parameters of the explanation model, for example, to weights of generated instances, to the number of the generated instances, etc.

The second approach consists of the well-known method SHAP (SHapley Additive exPlanations) [33, 50] and its modifications. The method is inspired by game-theoretic Shapley values [48] which can be interpreted as average expected marginal contributions over all possible subsets (coalitions) of features to the black-box model prediction. SHAP has many advantages, for example, it can be used for local and global explanations in contrast to LIME, but there are also two important shortcomings. The first one is a question how to add or remove features in order to implement their subsets as inputs for the black-box model. There are many approaches to removing features, exhaustively described by Covert et al. [16], but SHAP may be too sensitive to each of them, and there is no strong justifications of their use. Nevertheless, SHAP can be regarded as the most promising and efficient explanation method.

The second shortcoming is that SHAP is computationally expensive when there is a large number of features due to considering all possible coalitions whose number is 2^m , where m is the number of features. Therefore, the computational time grows exponentially. Several simplifica-

tions and approximations have been proposed in order to overcome this difficulty. Some of them are presented by Strumbelj and Kononenko [50, 51, 52]. One of the simplifications is based on using ordered permutations of the feature indices and probability distributions of features [51]. Another approximation is the quasi-random and adaptive sampling which includes two improvements [52]. The first one is based on exploiting Monte Carlo integration. The second improvement is based on the optimal number of perturbations of every feature in accordance with its variance to minimize the overall approximation error. Strumbelj and Kononenko [52] also proposed to average local contributions of values of each feature across all instances. Another interesting approach to simplify SHAP is the Kernel SHAP [33] which can be regarded as a computationally efficient approximation to Shapley values in higher dimensions. In order to relax the assumption of the feature independence accepted in Kernel SHAP, Aas et al. [1] extended the Kernel SHAP method to handle dependent features. Ancona et al. [4] proposed the polynomial-time approximation of Shapley values called the Deep Approximate Shapley Propagation (DASP) method.

In spite of many approaches to simplify SHAP, it is difficult to expect a significant simplification from the above modifications of SHAP. Therefore, a new approach is proposed for simplifying the SHAP method and for reducing computational expenses for calculating the Shapley values. A key idea behind the proposed approach is to apply a modification of the random subspace method [25] and to consider an ensemble of random SHAPs. The approach is very similar to the random forests when an ensemble of randomly built decision trees is used to get some average classification or regression measures. Random SHAPs are constructed by random selection of t features with indices $J_k = (i_1, \dots, i_t)$ from the instance for explanation and the obtained subset of the instance features is analyzed by SHAP as a separate instance. Repeating this procedure N times, we get a set $\mathcal{S} = \{S_1, \dots, S_N\}$ of the Shapley values corresponding to the input subsets of features, where the k -th subset is $S_k = \{\phi_i : i \in J_k\}$. By applying some combination rule for combining subsets S_k from \mathcal{S} , we obtain the final Shapley values.

The above general approach considering an ensemble of random SHAPs has several extensions which form the corresponding methods and algorithms. First of all, we can generate points around the analyzed instance and construct S_k for the k -th generated point. In this case, every point is assigned by a weight depending on the distance from the analyzed point. As a result, we can combine subsets S_k of the Shapley values with weights which are defined as a function of the distance from the analyzed point.

Another extension or modification is to select features in accordance with a probability distribution to get instances consisting of features with indices from the set J_k . Let us define the discrete probability distribution over the set of all indices. It can be produced, for example, by using the random forest [12] which plays a role of a feature selection model. At that, the random forest is constructed by using a set of points (instances) locally generated around the explained point. Every decision tree is built by using a single point from the set of generated points.

In sum, the contribution of the paper can be formulated as follows:

1. A new approach to implementing an ensemble-based SHAP with random subsets of features of the explained instance is proposed.
2. Several combination schemes are studied for aggregating subsets of important features obtained by using random SHAPs.

3. The approach is extended by generating random points in the local area around a test instance and computing subsets of important features separately for every point. A some kind of diversity is implemented with this extension.
4. Another extension is to use a probability distribution for the random selection of features defined by means of the random forest constructed by using the generated points in the local area around a test instance. The preliminary feature selection can be regarded as a pre-training procedure.

A lot of numerical experiments with an algorithm implementing the proposed method on synthetic and real datasets demonstrate its efficiency and properties for local and global interpretation.

The paper is organized as follows. Related work is in Section 2. The Shapley values and the SHAP method as a powerful tool for local and global explanations are introduced in Section 3. A detailed description of the proposed modifications of SHAP, including ER-SHAP, ERW-SHAP, ER-SHAP-RF is provided in Section 4. Numerical experiments with synthetic data and real data using the local interpretation by means of the proposed models and their comparison with the standard SHAP method are given in Section 5. Concluding remarks can be found in Section 6.

2 Related work

Local interpretation methods. An increasing importance of machine learning models and algorithms leads to development of new explanation methods taking into account various peculiarities of applied problems. As a result, many models of the local interpretation have been proposed. Success and simplicity of the LIME interpretation method resulted in development of several its modifications, for example, ALIME [47], Anchor LIME [42], LIME-Aleph [39], GraphLIME [26], SurvLIME [29], etc. A comprehensive analysis of LIME, including the study of its applicability to different data types, for example, text and image data, is provided by Garreau and Luxburg [21]. The same analysis for tabular data is proposed by the same authors [22]. An image version of LIME with its deep theoretical study is presented by Garreau and Mardaoui [20]. An interesting information-theoretic justification of interpretation methods on the basis of the concept of the explainable empirical risk minimization is proposed by Jung [27].

In order to relax the linearity condition for the local interpretation models like LIME and to adequately approximate a black-box model, several interpretation methods based on using Generalized Additive Models (GAMs) [24] were proposed [14, 32, 37, 59]. Another interesting class of models based on using a linear combination of neural networks such that a single feature is fed to each network was proposed by Agarwal et al. [3]. The impact of every feature on the prediction in these models is determined by its corresponding shape function obtained by each neural network. Following ideas behind these interpretation models, Konstantinov and Utkin [28] proposed a similar model. In contrast to the method proposed by Agarwal et al. [3], an ensemble of gradient boosting machines is used in [28] instead of neural networks in order to simplify the explanation model training process.

Another explanation method is SHAP [33, 50], which takes a game-theoretic approach for optimizing a regression loss function based on Shapley values. General questions of the compu-

tational efficiency of SHAP were investigated by Van den Broeck et al. [18]. Bowen and Ungar [11] proposed the generalized SHAP method (G-SHAP) which allows us to compute the feature importance of any function of a model’s output. Rozemberczki and Sarkar [44] presented an approach to applying SHAP to ensemble models. The problem of explaining the predictions of graph neural networks by using SHAP was considered by Yuan et al. [56]. Frye et al. [19] introduced the so-called off- and on-manifold Shapley values for high-dimensional multi-type data. Application of SHAP to explanation of recurrent neural networks was studied in [8]. Begley et al. present a new approach to explaining fairness in machine learning, based on the Shapley value paradigm. Antwarg et al. [5] study how to explain anomalies detected by autoencoders using SHAP. The problem of explaining anomalies detected by PCA is also considered by Takeishi [53]. Bouneder et al. [10] proposed X-SHAP which extends one of the approximations of SHAP called the Kernel SHAP [33]. SHAP is also applied to problems of explaining individual predictions when features are dependent [1] or when features are mixed [40]. SHAP has been used in real applications to explain predictions of the black-box models, for example, it was used to rank failure modes of reinforced concrete columns and to explain why a machine learning model predicts a specific failure mode for a given sample [34]. It was also used in chemoinformatics and medicinal chemistry [43]. An interesting application of SHAP in the desirable interpretation of the machine learning-based model results for identifying m7G sites in the gene expression analysis was proposed by Bi et al. [9]. Basic problems of SHAP are also analyzed by Kumar et al. [30].

Many other interpretation methods, their analysis, and critical reviews can be found also in survey papers [2, 6, 7, 13, 17, 23, 31, 45, 54].

3 Shapley values and the explanation model

One of the most powerful approaches to explaining predictions of the black-box machine learning models is the approach based on using the Shapley values [48] as a key concept in coalitional games. According to the concept, the total gain of a game is distributed to players such that desirable properties, including efficiency, symmetry, and linearity, are fulfilled. In the framework of the machine learning, the gain can be viewed as the machine learning model prediction or the model output, and a player is a feature of input data. Hence, contributions of features to the model prediction can be estimated by Shapley values. The i -th feature importance is defined by the Shapley value

$$\phi_i(f) = \phi_i = \sum_{S \subseteq N \setminus \{i\}} B(S, N) [f(S \cup \{i\}) - f(S)], \quad (1)$$

where $f(S)$ is the characteristic function in terms of coalitional games or the black-box model prediction under condition that a subset S of features are used as the corresponding input in terms of machine learning; N is the set of all features; $B(S, N)$ is defined as

$$B(S, N) = \frac{|S|! (|N| - |S| - 1)!}{|N|!}. \quad (2)$$

It can be seen from the above expression that the Shapley value ϕ_i can be regarded as the average contribution of the i -th feature across all possible permutations of the feature set.

The Shapley value has the following important properties:

Efficiency. The total gain is distributed as $\sum_{k=0}^m \phi_k = f(\mathbf{x})$.

Symmetry. If two players with numbers i and j make equal contributions, i.e., $f(S \cup \{i\}) = f(S \cup \{j\})$ for all subsets S which contain neither i nor j , then $\phi_i = \phi_j$.

Dummy. If a player makes zero contribution, i.e., $f(S \cup \{j\}) = f(S)$ for a player j and all $S \subseteq N \setminus \{j\}$, then $\phi_j = 0$.

Linearity. A linear combination of multiple games f_1, \dots, f_n , represented as $f(S) = \sum_{k=1}^n c_k f_k(S)$, has gains derived from f : $\phi_i(f) = \sum_{k=1}^n c_k \phi_i(f_k)$ for every i .

Let us consider a machine learning problem. Suppose that there is a dataset $\{(\mathbf{x}_1, y_1), \dots, (\mathbf{x}_n, y_n)\}$ of n points (\mathbf{x}_i, y_i) , where $\mathbf{x}_i \in \mathcal{X} \subset \mathbb{R}^m$ is a feature vector consisting of m features, y_i is the observed output for the feature vector \mathbf{x}_i such that $y_i \in \mathbb{R}$ in the regression problem and $y_i \in \{1, 2, \dots, T\}$ in the classification problem with T classes. If a task is to interpret or to explain the prediction from the model $f(\mathbf{x}^*)$ at a local feature vector \mathbf{x}^* , then the prediction $f(\mathbf{x}^*)$ can be represented by using Shapley values as follows [33, 50]:

$$f(\mathbf{x}^*) = \phi_0 + \sum_{j=0}^m \phi_j^*, \quad (3)$$

where $\phi_0 = \mathbb{E}[f(\mathbf{x})]$, ϕ_j^* is the value ϕ_j for the prediction $\mathbf{x} = \mathbf{x}^*$.

The above implies that the Shapley values explain the difference between the prediction $f(\mathbf{x}^*)$ and the global average prediction.

One of the crucial questions for implementing the SHAP method is how to remove features from subset $N \setminus S$, i.e., how to fill input features from subset $N \setminus S$ in order to get predictions $f(S)$ of the black-box model. A detailed description of various ways for removing features is presented by Covert et al. [16]. One of the ways is simply by setting the removed features to zero [38, 58] or by setting them to user-defined default values [41]. According to the way, features are often replaced with their mean values. Another way removes feature by replacing them with a sample from a conditional generative model [55]. In the LIME method for tabular data, features are replaced with independent draws from specific distributions [16] such that each distribution depends on original feature values. These are only a part of all ways for removing features.

4 Modifications of SHAP

4.1 ER-SHAP

In spite of many approaches to simplify SHAP, it is difficult to expect a significant simplification from the above modifications of SHAP. Therefore, a new approach is proposed for simplifying the SHAP method and for reducing computational expenses for calculating the Shapley values. A key idea behind the proposed approach is to apply a modification of the random subspace method [25] and to consider an ensemble of random SHAPs. The approach is very similar to the random forests when an ensemble of randomly built decision trees is used to get some average classification or regression measures.

Suppose that instance $\mathbf{x} \in \mathbb{R}^m$ has to be interpreted under condition that the black-box model has been trained on the dataset $D = \{(\mathbf{x}_1, y_1), \dots, (\mathbf{x}_n, y_n)\}$. A general scheme of the first approach

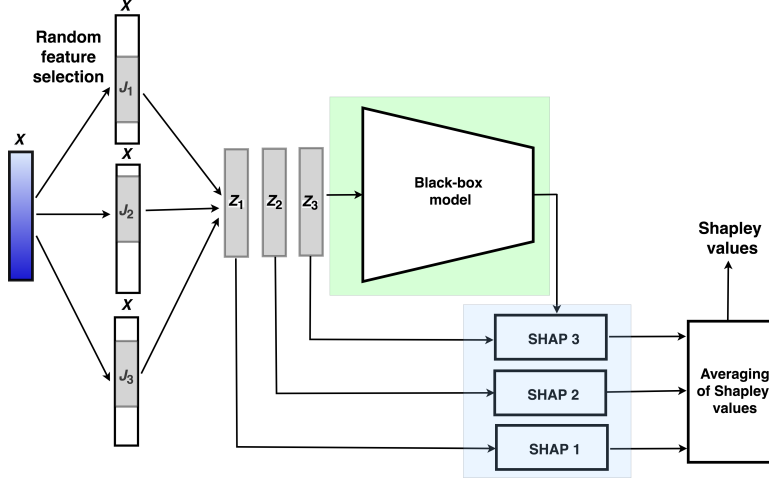


Figure 1: A scheme of the ER-SHAP

called Ensemble of Random SHAPs (ER-SHAP) for case $N = 3$ is illustrated in Fig. 1. ER-SHAP is iteratively constructed by random selection of t different features N times. Value t is a training parameter. If we refer to random forests, then one of the heuristics is $t \approx \sqrt{m}$. However, the optimal t is obtained by considering many its values. Suppose that indices of selected features at the k -th iteration form the set $J_k = (i_1, \dots, i_t)$. The corresponding vector of t features is regarded as an instance $\mathbf{z}_k = (x_{i_1}, \dots, x_{i_t}) \in \mathbb{R}^t$. Subsets of selected features with indices J_k are shown in Fig. 1 as successive features. However, this is only a schematic illustration. Features are randomly selected in accordance with the uniform distribution and can be located at arbitrary places of vector \mathbf{x} .

As a result, we have a set of N instances $\mathbf{z}_1, \dots, \mathbf{z}_N$. The next step is to use the black-box model and SHAP to compute Shapley values for every instance such that the subset $S_k = \{\phi_i^{(k)} : i \in J_k\}$ of the Shapley values $\phi_i^{(k)}$ is produced for instance \mathbf{z}_k . Repeating this procedure N times, we get a set $\mathcal{S} = \{S_1, \dots, S_N\}$ of the Shapley values corresponding to all \mathbf{z}_k , $k = 1, \dots, N$, or all input subsets of features. Having set \mathcal{S} , we can apply several combination rules to combining subsets S_k from \mathcal{S} . One of the simplest rules is based on averaging of the Shapley values over all subsets S_k :

$$\phi_i = \frac{1}{N_i} \sum_{k: i \in J_k} \phi_i^{(k)}, \quad i = 1, \dots, m, \quad (4)$$

where N_i is the number of the i -th feature selections among all iterations, i.e. $N_i = \sum_{k: i \in J_k} 1$.

It should be noted that the input of the black-box model has to have m features. Therefore, for performing SHAPs with every \mathbf{z}_k , average values of features over all dataset D are used to fill $m - t$ remain features though other methods [16] can be also used to fill these features.

Algorithm 1 can be viewed as a formal scheme implementing ER-SHAP. It is supposed that the black-box model has been already trained.

If the number of subsets S in the standard SHAP or the number of differences $f(S \cup \{i\}) -$

Algorithm 1 ER-SHAP

Require: Training set D ; point of interest \mathbf{x} ; the number of iterations N ; the number of selected features t ; the black-box model for explaining $f(\mathbf{x})$

Ensure: The Shapley values $S = \{\phi_1, \dots, \phi_m\}$

- 1: **for** $k = 1, k \leq N$ **do**
 - 2: Select randomly t features from \mathbf{x} and form the set J_k of indices of randomly selected features $x_i, i \in J_k$
 - 3: Use SHAP for computing $\phi_i^{(k)}, i \in J_k$ and form the set $S_k = \{\phi_i^{(k)} : i \in J_k\}$
 - 4: **end for**
 - 5: Combine sets $S_k, k = 1, \dots, N$, to compute S , for example, by using a simple averaging:
 $\phi_i = N_i^{-1} \sum_{k:i \in J_k} \phi_i^{(k)}$, where $N_i = \sum_{k:i \in J_k} 1$.
-

$f(S)$, which have to be computed is 2^m , then the number of the same differences in ER-SHAP is $N \cdot 2^t$. For comparison purposes, if we consider a dataset with $m = 25$ and $t = \sqrt{m} = 5$, then N can be taken $2^{25}/2^5 = 2^{20}$ in order to make equal computational complexity of SHAP and ER-SHAP.

4.2 ERW-SHAP

The next algorithm is called the Ensemble of Random Weighted SHAPs (ERW-SHAP) algorithm differs from ER-SHAP in the following parts. A general scheme is shown in Fig. 2. First of all, N points $\mathbf{h}_1, \dots, \mathbf{h}_N$ are generated in the neighborhood of explained instance \mathbf{x} . These points do not need to belong to the dataset D . Then t features are randomly selected from every \mathbf{h}_k , and they produce instances $\mathbf{z}_1, \dots, \mathbf{z}_N$. Moreover, the weight w_k of each instance \mathbf{h}_k is defined as a function of the distance d_k between the explained instance \mathbf{x} and the generated neighbor \mathbf{h}_k . The weights are used to implement the weighted average of the Shapley values. The final Shapley values are calculated now as follows:

$$\phi_i = \frac{1}{W_i} \sum_{k:i \in J_k} w_k \phi_i^{(k)}, \quad i = 1, \dots, m, \quad (5)$$

where $W_i = \sum_{k:i \in J_k} w_k$.

On the one hand, using these changes of ER-SHAP, we implement an idea of some kind of diversity of SHAPs to make the randomly selected feature vectors more independent. On the other hand, the approach is similar to the LIME method where the analyzed instance is perturbed in order to build an approximating linear model around the instance to be explained. The diversity of SHAPs is a very important peculiarity of the proposed ER-SHAP. It prevents SHAP from the situation when a rule for filling the removed features produces features coinciding with the explained instance features. In this case, the Shapley values are incorrectly computed. The use of generated neighbors allows us to avoid this case and to get more accurate results.

Algorithm implementing ERW-SHAP differs from the similar Algorithm 1 implementing EW-SHAP only in two lines. First, after line 1 or before line 2, the line indicating how to generate neighbors has to be inserted. Second, line 5 (combination of the Shapley values) is replaced with expression (5).

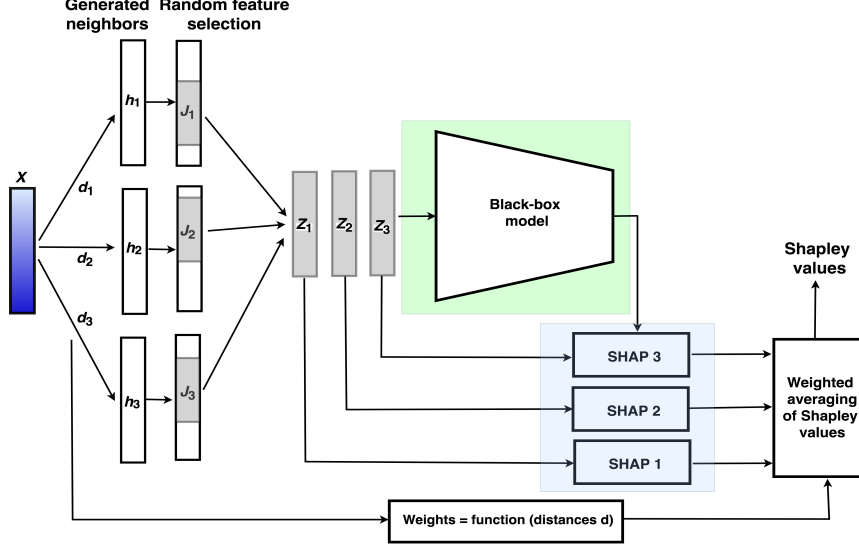


Figure 2: A scheme of the ERW-SHAP

4.3 ER-SHAP-RF

In order to control the process of the random feature selection, it is reasonable to choose features for producing z_1, \dots, z_N in accordance with some probability distribution different from the uniform distribution, which would take into account the preliminary importance of features. The intuition behind this modification is to reduce the selection of unimportant features which do not impact on the black-box prediction corresponding to x a priori.

One of the ways to implement this control is to compute the preliminary feature importance by means of the random forest. Although it is known that the random forest does not always give acceptable results related to the feature selection problem, the proposed approach does not have this drawback because we propose to train the random forest on instances generated in the neighborhood of explained instance x . The next algorithm is called the Ensemble of Random SHAPs generated by the Random Forest (ER-SHAP-RF) algorithm. The random forest plays a role of the important feature selection model. It can be also viewed as some kind pre-training for important features. The idea to train the random forest on generated neighbors allows us to implement an preliminary explanation method. It should be noted that the random forest is not a unique model for selecting important features. There are many methods [49], which could be used for solving this task. We use the random forest as one of the popular and simple methods having a few parameters. In the same way, the linear regression model could be used instead of the random forest. The random forest can be used as a explanation model by applying an approach proposed by Sagi and Rokach [46] based on a scalable method for transforming a decision forest into a single decision tree which is interpretable.

The LIME method can be also applied to get the probability distribution of features. In the case of its use, normalized absolute values of linear regression coefficients can be regarded as the

probability distribution of features.

For solving the feature selection task by random forests, we use the well-known simple method [12]. According to this method, for every tree from the random forest, we compute how much the impurity is decreased by a feature. The more the feature decreases the impurity, the more important the feature is. The impurity decreasing is averaged across all trees in the random forest, and the obtained value corresponds to the final importance of the feature.

The proposed approach may leads to small probabilities of unimportant features. However, it does not mean that these features will not selected for using in explanation by means of SHAP. They have a smaller chance to be selected under condition that their probabilities are not equal to zero. This implies that the classification or regression models for constructing the probability distribution P should not provide some sparse predictions like the Lasso because only a small part of features in this case will take part in explanation.

A general scheme of ER-SHAP-RF is shown in Fig. 3 where a number, say M , of neighbors $\mathbf{h}_1, \dots, \mathbf{h}_M$ are generated around the instance \mathbf{x} to be explained. Every generated neighbor \mathbf{h}_j is fed into the black-box model to get its class label y_j^* . It should be noted that the training instances can be taken as neighbors. However, they should be classified by using the black-box model in order to take into account this model in explanation.

Having the obtained training with points (\mathbf{h}_j, y_j^*) , we train the random forest which provides the feature importance measure in the form of the probability distribution $P = (p_1, \dots, p_m)$. The distribution P is used to select features from instance \mathbf{x} for constructing the vectors $\mathbf{z}_1, \dots, \mathbf{z}_N$, namely, t features are selected from \mathbf{x} with replacement N times in accordance with the distribution P . SHAPs are used to find the Shapley values of vectors $\mathbf{z}_1, \dots, \mathbf{z}_N$. They are combined similarly to ERW-SHAP by means of averaging as follows:

$$\phi_i = \frac{1}{N_i} \sum_{k:i \in J_k} \phi_i^{(k)}, \quad i = 1, \dots, m. \quad (6)$$

It is important that the number N_i of the i -th feature selections among all iterations N is used instead of N .

The random forest should be built with a large depth of trees and with a small number of trees in order to avoid a rather sparse probability distribution of features when a large part of probabilities will be equal to zero or close to zero. Another way for avoiding small probabilities of features is to apply calibration methods and to recalculate the obtained probabilities, for example, by using the temperature scaling as the simplest extension of Platt scaling [15]:

$$p_k^* = \frac{\exp(p_k/T)}{\sum_{i=1}^m \exp(p_i/T)}, \quad k = 1, \dots, m, \quad (7)$$

where T is the temperature which controls the smoothness of the probability distribution, but it does not change the maximum of the softmax function.

Algorithm 2 implementing ER-SHAP-RW can be viewed as an extension of ER-SHAP.

It is interesting to point out that the fourth algorithm can be also proposed, which is represented as a combination of ERW-SHAP and ER-SHAP-RF. N points are generated for implementing diversity in accordance with ERW-SHAP, and M points are generated for training the

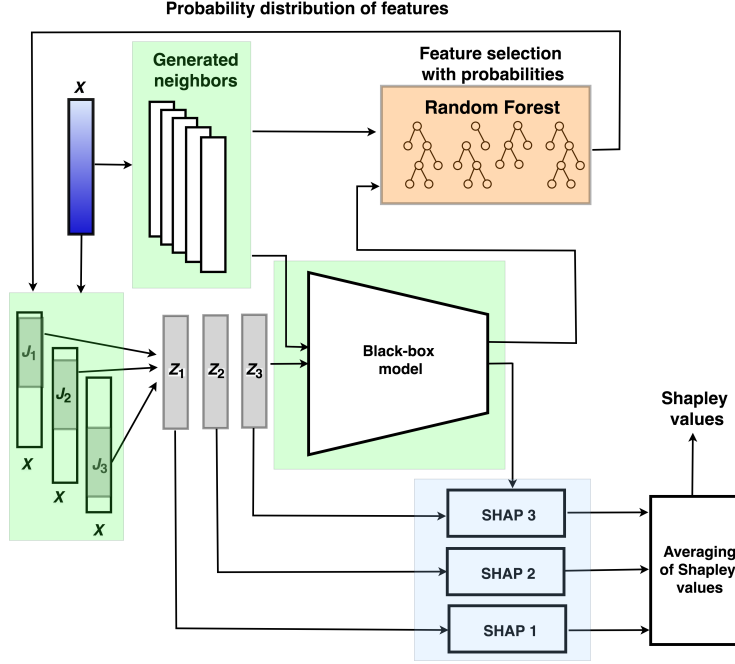


Figure 3: A scheme of the ER-SHAP-RF

Algorithm 2 ER-SHAP-RF

Require: Training set D ; point of interest \mathbf{x} ; the number of iterations N ; the number of selected features t ; the black-box model for explaining $f(\mathbf{x})$; parameters of the random forest (the number and depth of trees, number of instances for building trees)

Ensure: The Shapley values $S = \{\phi_1, \dots, \phi_m\}$

- 1: Generate M instances $\mathbf{h}_1, \dots, \mathbf{h}_M$ which are from the neighborhood of \mathbf{x} or from the whole training set
 - 2: Compute the class label $y_j^* = f(\mathbf{h}_j)$ for every generated instance by using the black-box model
 - 3: Train the random forest on (\mathbf{h}_j, y_j^*) , $j = 1, \dots, M$
 - 4: Compute the probability distribution P of features by using the random forest
 - 5: **for** $k = 1$, $k \leq N$ **do**
 - 6: Select randomly t features from \mathbf{x} in accordance with the probability distribution P and form the index set J_k of features
 - 7: Use SHAP for computing $\phi_i^{(k)}$, $i \in J_k$ and form the set $S_k = \{\phi_i^{(k)} : i \in J_k\}$
 - 8: **end for**
 - 9: Combine sets S_k , $k = 1, \dots, N$, to compute S , for example, by using a simple averaging:

$$\phi_i = N_i^{-1} \sum_{k: i \in J_k} \phi_i^{(k)}, \text{ where } N_i = \sum_{k: i \in J_k} 1.$$
-

random forest in accordance with ER-SHAP-RF and for computing the prior probability distribution P of features. Then the random features are selected not from the vector \mathbf{x} as it is done in ER-SHAP-RF, but from every vector \mathbf{h}_k with the probability distribution P , $k = 1, \dots, N$. However, this algorithm is not studied because it can be regarded as the combination of ERW-SHAP and ER-SHAP-RF, which are analyzed in detail.

5 Numerical experiments

First, we consider several numerical examples for which training instances are randomly generated. Each generated synthetic instance consists of 5 features. Two features are generated as shown in Fig. 4, and other features are uniformly generated in intervals $[-1, 1]$. Each picture in Fig. 4 corresponds to a certain location of instances of two classes such that the instances of classes 0 and 1 are depicted by small triangles and crosses, respectively. This generation corresponds to the case when the first two features may be important. These features allow us to analyze the feature importance in accordance with the data location and with the separating function. Other features are not important, and they are used to generalize numerical experiments with synthetic data.

Separating functions in Fig. 4 are obtained by means of SVM which can be regarded as the black-box model. It used the RBF kernel whose parameter depends on a dataset trained. The SVM allows us to get different separating functions by changing the kernel parameter. Fig. 4(a) illustrates the linearly separating case. The specific class area in the form of a stripe is shown in Fig. 4(b). A saw-based separating function is used in Fig. 4(c). The class area in the form of a wedge is given in Fig. 4(d). A checkerboard with an attempt of SVM to separate the checkerboard cages can be found in Fig. 4(e). For every generated dataset from Fig. 4, we compare SHAP with the proposed modifications.

Measures for comparison: In order to compare the proposed modifications with the original SHAP method, we use the concordance index C of pairs, which is defined as the proportion of concordant pairs of the Shapley values divided by the total number of possible evaluation pairs. Let ϕ_i^* and ϕ_i be the Shapley values obtained by means of the original SHAP method and one of its modifications (ER-SHAP, ERW-SHAP, ER-SHAP-RF), respectively. Two pairs of the Shapley values (ϕ_i, ϕ_j) and (ϕ_i^*, ϕ_j^*) are concordant if there hold $(\phi_i > \phi_j, \phi_i^* > \phi_j^*)$ or $(\phi_i < \phi_j, \phi_i^* < \phi_j^*)$. In contrast to the well-known C-index in survival analysis, the introduced concordance index compares predictions provided by two methods. If the index is close to 1, then the models provide the same results. A motivation for the concordance index introduction is that the Shapley values computed by using original SHAP and the proposed modifications may be different. However, we are interesting in their relationship. If the original SHAP method give the inequality $\phi_i^* > \phi_j^*$ for some i and j , then we are expecting to have $\phi_i > \phi_j$ for the proposed method, but not equalities $\phi_i^* = \phi_i$ and $\phi_j^* = \phi_j$. It should be noted that original SHAP may provide incorrect results. Therefore, the introduced concordance index should be viewed as a desirable measure under condition of correct SHAP results.

We use the Kernel SHAP [33] in numerical experiments and compare obtained results with it.

In spite of importance of the concordance index, we also use the normalized Euclidean distance E between vectors $(\phi_1^*, \dots, \phi_m^*)$ and (ϕ_1, \dots, ϕ_m) . The distance shows how the absolute Shapley

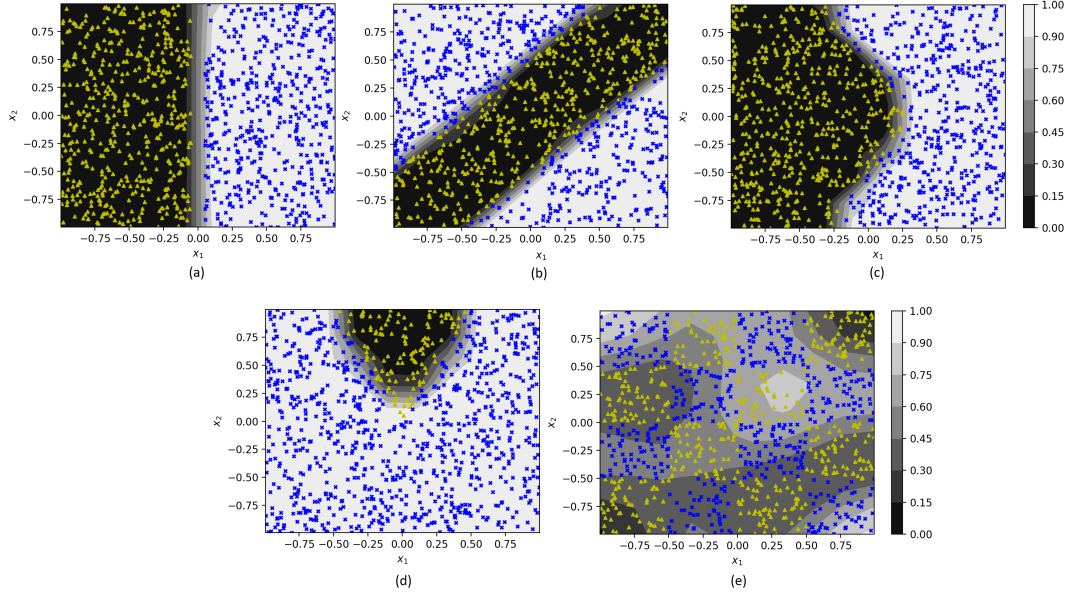


Figure 4: Five synthetic datasets and the boundaries between classes provided by SVM

values of two methods are close to each other. It is important to take into account that the Shapley values in the original SHAP method satisfy the efficiency property when $\phi_1^* + \dots + \phi_m^* = f(\mathbf{x}) - f(\emptyset)$. This property is not fulfilled for modifications because they do not enumerate all subsets of features. Therefore, in order to consider the Shapley values in the same scale, all values ϕ_i and ϕ_i^* are normalized to be in interval $[0, 1]$.

5.1 ER-SHAP

First, we consider results of numerical experiments obtained by means of ER-SHAP with the SVM as a black-box model trained on the datasets shown in Fig. 4. The explained instance for experiments has all identical features which are equal to 0.25. The concordance indices of ER-SHAP as functions of the number of iterations N for the numbers of selected features $t = 2$ (the solid line) and $t = 3$ (the dashed line) are illustrated in Fig. 5, where pictures (a)-(e) correspond to pictures (a)-(e) shown in Fig. 4. It can be seen from Fig. 5 that the concordance index increases with N on average. This implies that ER-SHAP provides results comparable with SHAP. It can be also seen from pictures that the concordance index is significantly larger for $t = 3$ in comparison with the case of $t = 2$. This observation is obvious because the large number of selected features in each iteration brings the modification closer the original SHAP method. Though one can see from Fig. 5 (b) that the case $t = 2$ provides better concordance index by $N \geq 7$.

Fig. 6 illustrates how the Euclidean distances between ER-SHAP and SHAP as functions of the number of iterations N for $t = 2$ (the solid line) and 3 (the dashed line) decrease with N . We

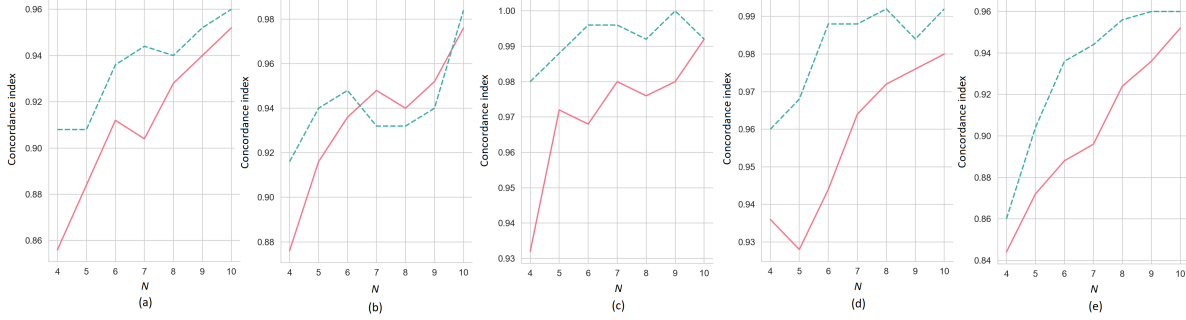


Figure 5: Concordance indices of ER-SHAP as functions of the number of iterations N for $t = 2$ (the solid line) and 3 (the dashed line) and for five datasets and trained SVMs

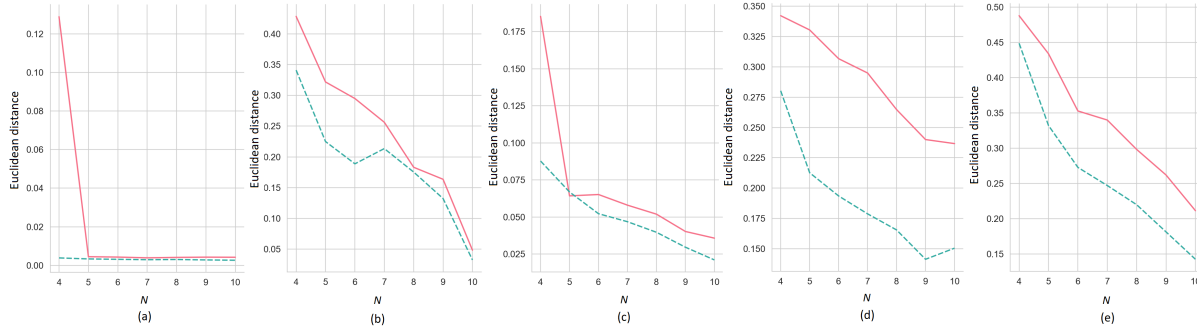


Figure 6: Euclidean distances between ER-SHAP and SHAP as functions of the number of iterations N for $t = 2$ (the solid line) and 3 (the dashed line) and for five datasets and trained SVMs

again consider five training sets shown in Fig. 4.

In order to explicitly illustrate how the Shapley values ϕ_i^* and ϕ_i obtained by SHAP and ER-SHAP, respectively, are close to each other, we show the Shapley values for all five cases in Fig. 7. It can be seen that despite the difference in absolute values, the Shapley values indicate on the same important features.

5.2 ERW-SHAP

To study ERW-SHAP, features of the explained instance are noised by using the normal distribution of noise with the zero expectation and standard deviations 0.01 and 0.1. Weights of generated instances \mathbf{h}_i are defined by

$$w_i = \exp\left(-\|\mathbf{h}_i - \mathbf{x}\|^2\right). \quad (8)$$

We consider similar results of numerical experiments obtained by means of ERW-SHAP with the SVM as a black-box model trained on the datasets shown in Fig. 4 with the same explained

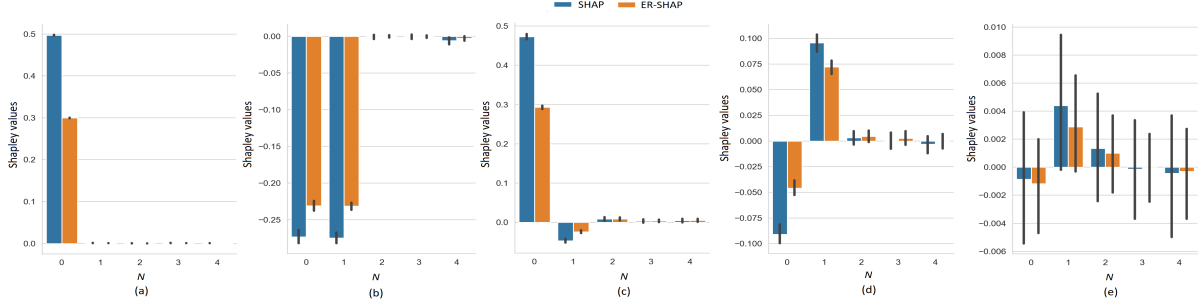


Figure 7: Shapley values obtained by means of SHAP and ER-SHAP as functions of the number of iterations N for five datasets and trained SVMs

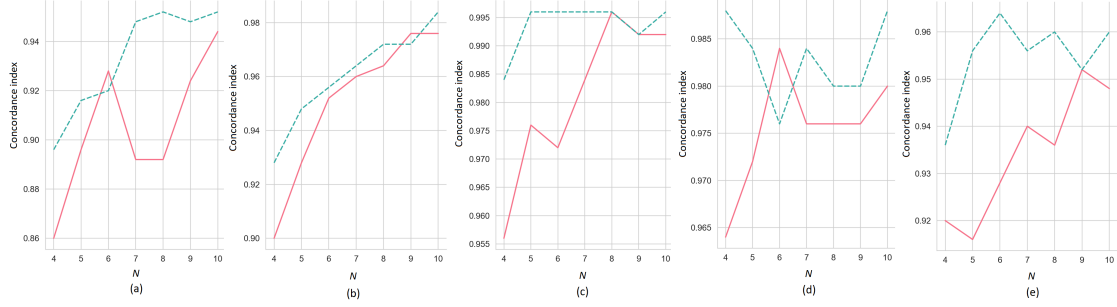


Figure 8: Concordance indices of ERW-SHAP as functions of N for $t = 2$ (the solid line) and 3 (the dashed line) and for five datasets and trained SVMs

instance. The concordance indices of ERW-SHAP as functions of N for $t = 2$ (the solid line) and $t = 3$ (the dashed line) are illustrated in Fig. 8, where pictures (a)-(e) correspond to pictures (a)-(e) shown in Fig. 4. The standard deviation of the normal distribution generating noise is 0.01. If we compare the concordance indices for ERW-SHAP (Fig. 8) and for ER-SHAP (Fig. 5), then it is obvious that ERW-SHAP provides better results in comparison with ER-SHAP for most datasets.

At the same time, the Euclidean distances between SHAP and ERW-SHAP slightly differ from the same distances between SHAP and ER-SHAP. This follows from Fig. 9 where Euclidean distances between ERW-SHAP and SHAP as functions of N for $t = 2$ (the solid line) and 3 (the dashed line) are presented for the above datasets.

To illustrate how the Shapley values ϕ_i^* and ϕ_i obtained by SHAP and ERW-SHAP, respectively, are close to each other, we show the Shapley values for five cases in Fig. 10 and in Fig. 11. Figs. 10 and 11 provide results under condition that the normal distribution of the generated noise has the standard deviations 0.1 and 0.01, respectively. We again observe that ERW-SHAP can be regarded as a good approximation of SHAP because Shapley values of ERW-SHAP and SHAP are very close to each other.

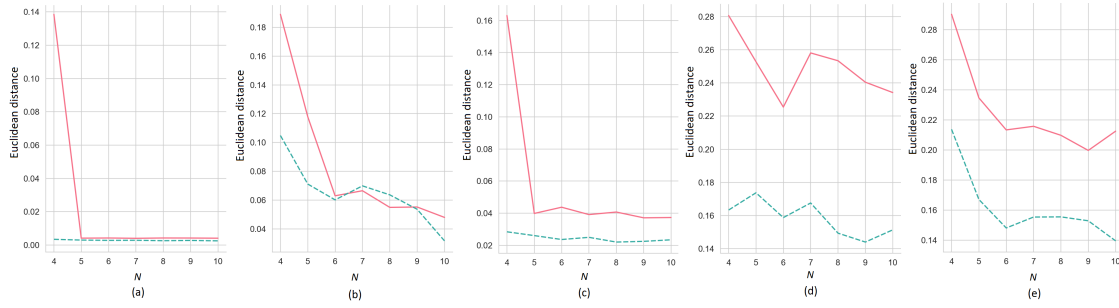


Figure 9: Euclidean distances between ERW-SHAP and SHAP as functions of N for $t = 2$ (the solid line) and 3 (the dashed line) and for five datasets and trained SVMs

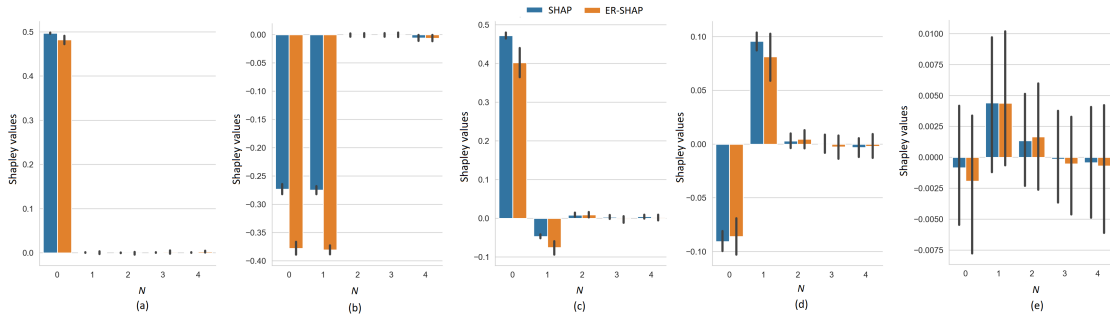


Figure 10: Shapley values obtained by means of SHAP and ERW-SHAP as functions of the number of iterations N for five datasets and trained SVMs under condition of using the normal distribution of feature changes with the standard deviation 0.1

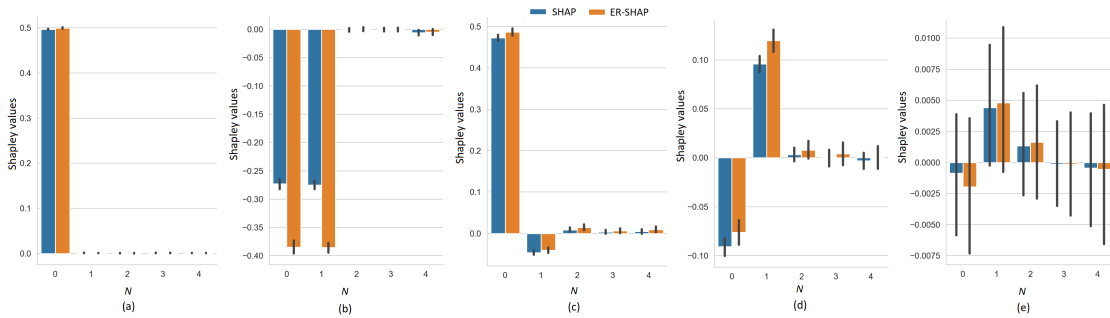


Figure 11: Shapley values obtained by means of SHAP and ERW-SHAP as functions of the number of iterations N for five datasets and trained SVMs under condition of using the normal distribution of feature changes with the standard deviation 0.01

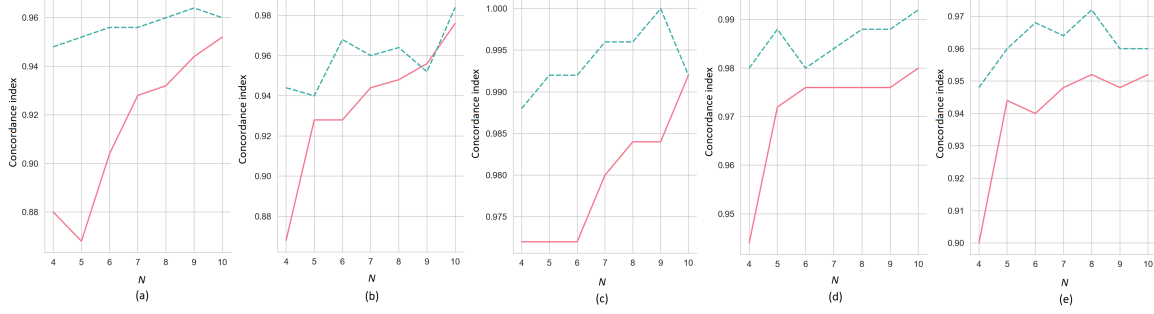


Figure 12: Concordance indices of ER-SHAP-RF as functions of N for $t = 2$ (the solid line) and 3 (the dashed line) and for five datasets and trained SVMs

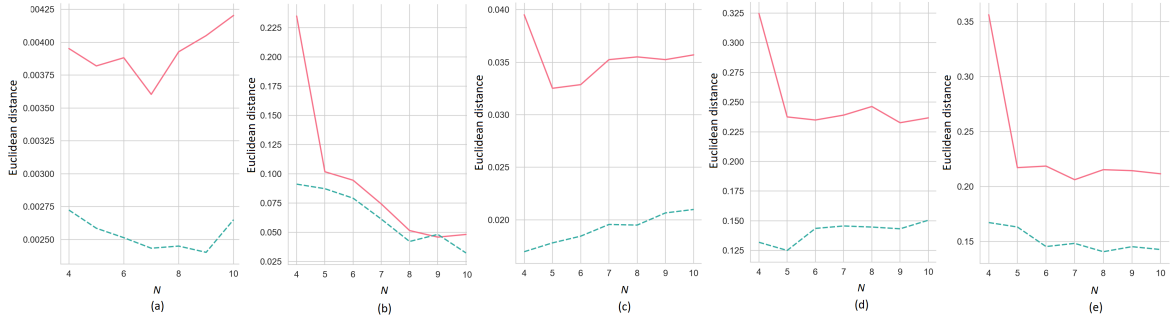


Figure 13: Euclidean distances between ER-SHAP-RF and SHAP as functions of N for $t = 2$ (the solid line) and 3 (the dashed line) and for five datasets and trained SVMs

5.3 ER-SHAP-RF

We again study the modification by using datasets shown in Fig. 4. The result show that ER-SHAP-RF outperforms ER-SHAP as well as ERW-SHAP for most dataset. Indeed, if we compare concordance indices for ER-SHAP-RF (Fig. 12) with ERW-SHAP (Fig. 8) and ER-SHAP (Fig. 5), then we see that all examples provide better results. In contrast to concordance indices, Euclidean distances shown in Fig. 13 demonstrate worse results. At the same time, Shapley values given in Fig. 14 almost coincide with the corresponding values obtained by means of the ERW-SHAP (Fig. 11). It should be noted that a more accurate tuning of the random forest might provide outperforming results.

5.4 Boston Housing dataset

Let us consider the real data called the Boston Housing dataset. It can be obtained from the StatLib archive (<http://lib.stat.cmu.edu/datasets/boston>). The Boston Housing dataset consists of 506 instances such that each instance is described by 13 features.

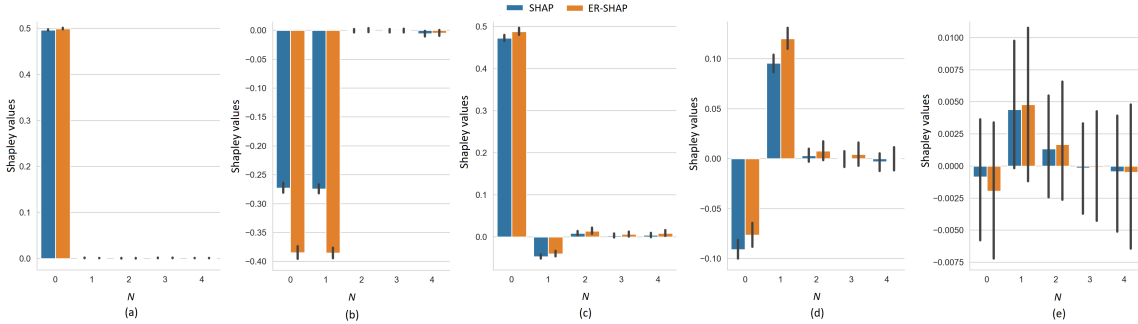


Figure 14: Shapley values obtained by means of SHAP and ER-SHAP-RF as functions of N for five datasets and trained SVMs

The heatmap reflecting the concordance index of ER-SHAP for the Boston Housing dataset is shown in Fig. 15. Each element at position (i, j) , where i and j are numbers of the row and column, respectively, indicates the value the concordance index. Each row corresponds to the number of iterations N , each column corresponds to the number of selected features t . It can be seen from Fig. 15 that the concordance index increases with N and t . This implies that ER-SHAP provides results coinciding with SHAP by rather large numbers of iterations N . Fig. 16 illustrates how the computation time τ_{SHAP} of SHAP exceeds the computation time $\tau_{\text{ER-SHAP}}$ of ER-SHAP. The heatmap shows the ratio $\tau_{\text{ER-SHAP}}/\tau_{\text{SHAP}}$. One can see from Fig. 16 a clear advantage of using ER-SHAP from the computational point of view.

Fig. 17 shows the heatmap of the concordance index of ERW-SHAP for the Boston Housing dataset. It is clearly seen from Fig. 17 that the introduction of weights and generated instances significantly improves the approximation.

Shapley values obtained by means of ER-SHAP and SHAP as well as ERW-SHAP and SHAP are shown in Figs. 18 and 19, respectively. One can see from Figs. 18 and 19 that ERW-SHAP can be viewed as a better approximation of SHAP because the corresponding bars almost coincide as shown in Fig. 19. It should be noted that Shapley values provided by ER-SHAP are also behaves like values of SHAP (see Fig. 18), but they do not coincide for the most important features.

Figs. 20 and 21 illustrate heatmaps of the concordance index of ER-SHAP-RF for the Boston Housing dataset. They are obtained without using the temperature scaling in accordance with (7) and with this calibration method, respectively. It is interesting to observe from Figs. 20 and 21 that the use of the calibration leads to a more contrasting heatmap and to obvious improvement of the approximation quality.

5.5 Breast Cancer dataset

The next real dataset is the Breast Cancer Wisconsin (Diagnostic). It can be found in the well-known UCI Machine Learning Repository (<https://archive.ics.uci.edu>). The Breast Cancer dataset contains 569 instances such that each instance is described by 30 features. For classes of the breast cancer diagnosis, the malignant and the benign are assigned by classes 0 and 1,

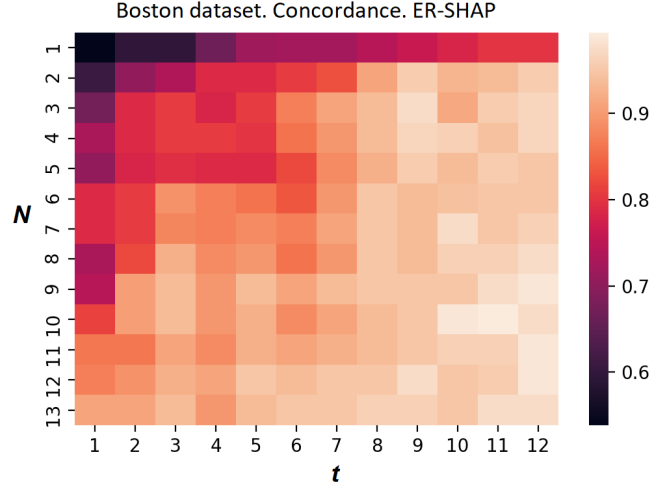


Figure 15: The heatmap reflecting the concordance index C obtained by ER-SHAP for the Boston Housing dataset

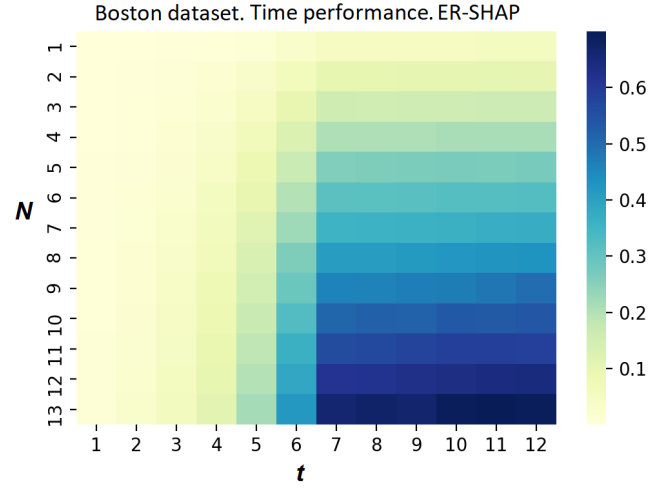


Figure 16: The heatmap illustrating the relationship between computation times of SHAP and ER-SHAP for the Boston Housing dataset

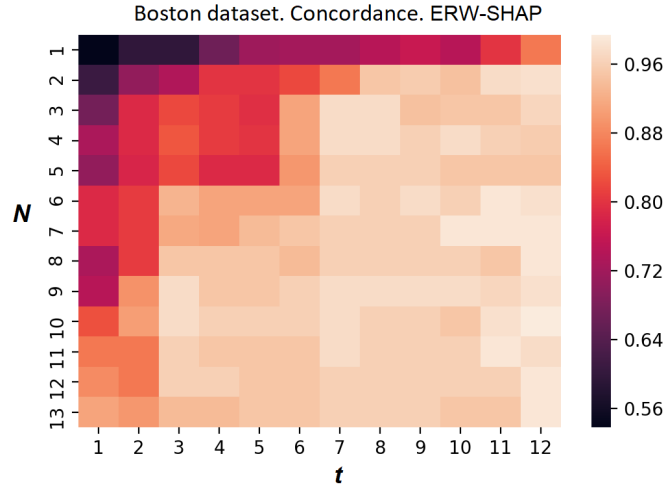


Figure 17: The heatmap reflecting the concordance index C obtained by ERW-SHAP for the Boston Housing dataset

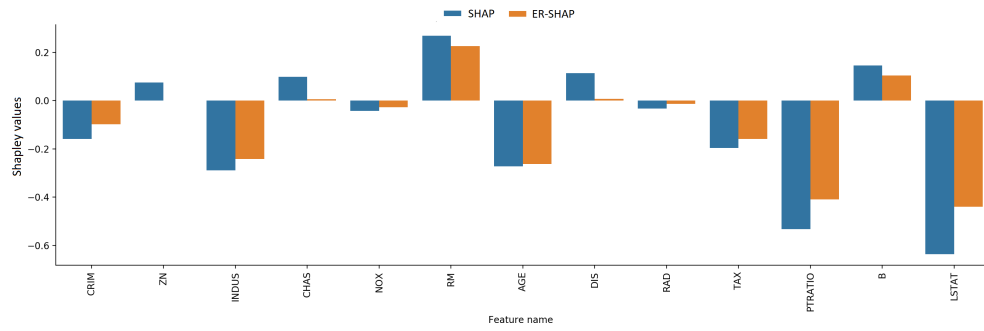


Figure 18: Shapley values obtained by means of SHAP and ER-SHAP as functions of N for the Boston Housing dataset

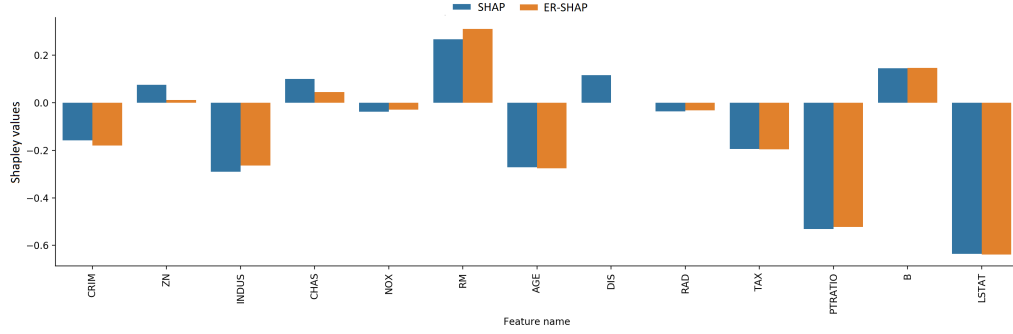


Figure 19: Shapley values obtained by means of SHAP and ERW-SHAP as functions of N for the Boston Housing dataset under condition of using the normal distribution of feature changes with the standard deviation 0.1

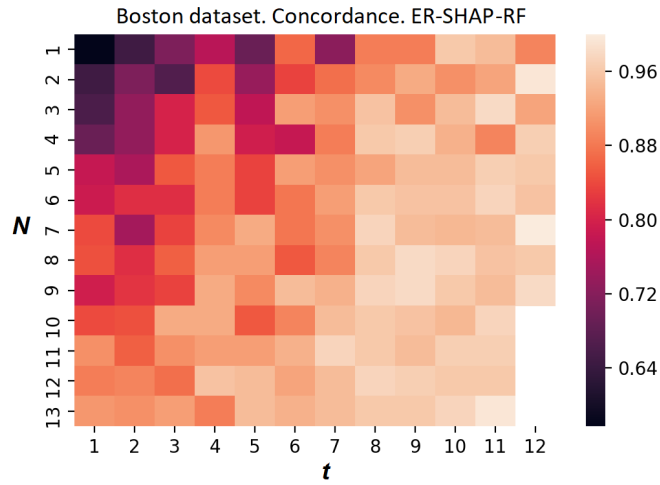


Figure 20: The heatmap reflecting the concordance index C obtained by ER-SHAP-RF for the Boston Housing dataset without using the temperature scaling

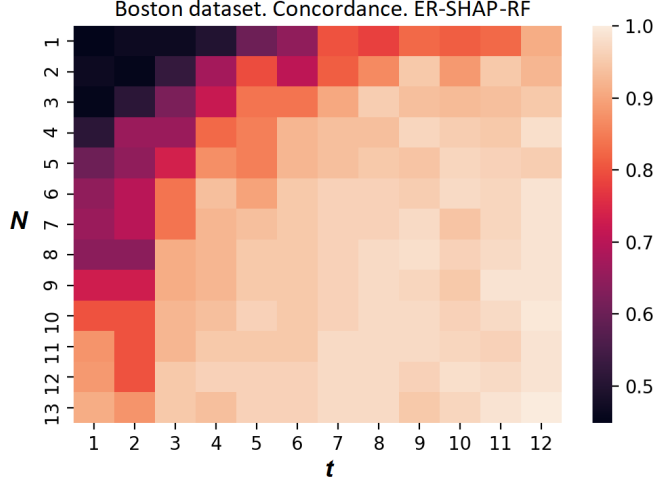


Figure 21: The heatmap reflecting the concordance index C obtained by ER-SHAP-RF for the Boston Housing dataset with using the temperature scaling

respectively. We consider the corresponding model in the framework of regression with outcomes in the form of probabilities from 0 (malignant) to 1 (benign).

Heatmaps given in Figs. 22-23 are similar to the same heatmaps obtained for the Boston Housing dataset (Figs. 15-16). It is interesting to observe from Fig. 23 that there are N and t such that the ratio $\tau_{\text{ER-SHAP}}/\tau_{\text{SHAP}}$ is larger 1. This implies that SHAP is computationally simpler in comparison with ER-SHAP. However, these cases take place only for large values N and t .

At first glance, it is difficult to evaluate from Fig. 24 whether ERW-SHAP provides better results than ER-SHAP. Fig. 24 shows the heatmap of the concordance index of ERW-SHAP for the Breast Cancer dataset. However, we can be that the legend in Fig. 24 is changed in interval $[0.4, 0.95]$, whereas the legend in Fig. 22 is changed in interval $[0.4, 0.9]$. This implies that ERW-SHAP outperforms ER-SHAP in this numerical example.

Shapley values for all features of the Breast Cancer dataset, which are obtained by means of ER-SHAP and SHAP, are shown in Fig. 25. Similar values obtained by means of ERW-SHAP and SHAP are shown in Fig. 19. One can see from Figs. 25 and 19 that the Shapley values obtained by means of ERW-SHAP better approximate the SHAP Shapley values. For example, if to look at the feature “worst radius”, which is important due to the original SHAP method, then ER-SHAP provides the incorrect result whereas ERW-SHAP is totally consistent with SHAP.

Figs. 27 and 28 illustrate heatmaps of the concordance index of ER-SHAP-RF for the Breast Cancer dataset. They show results similar to the results obtained for the Boston Housing dataset demonstrated in Figs. 20 and 21, respectively. This implies that the use of “pre-training” in the form of the random forest combined with the calibration method leads to better approximation.

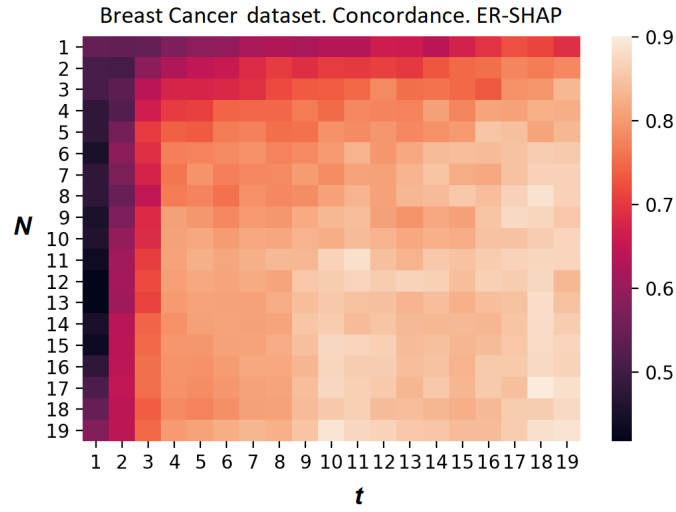


Figure 22: The heatmap reflecting the concordance index C obtained by ER-SHAP for the Breast Cancer dataset

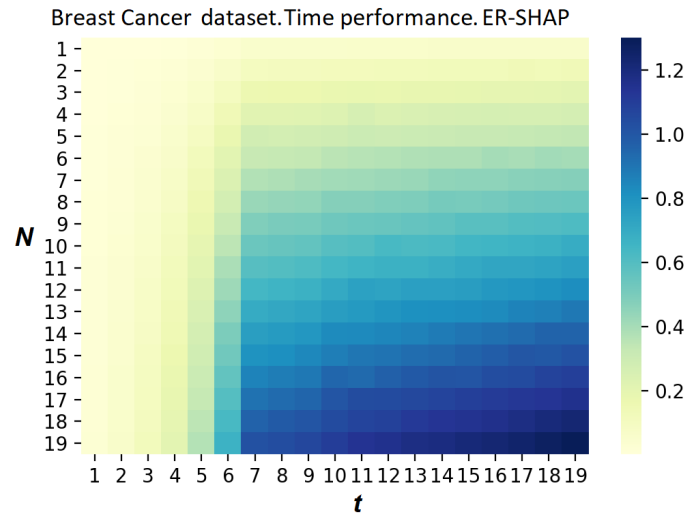


Figure 23: The heatmap illustrating the relationship between computation times of SHAP and ER-SHAP for the Breast Cancer Housing dataset

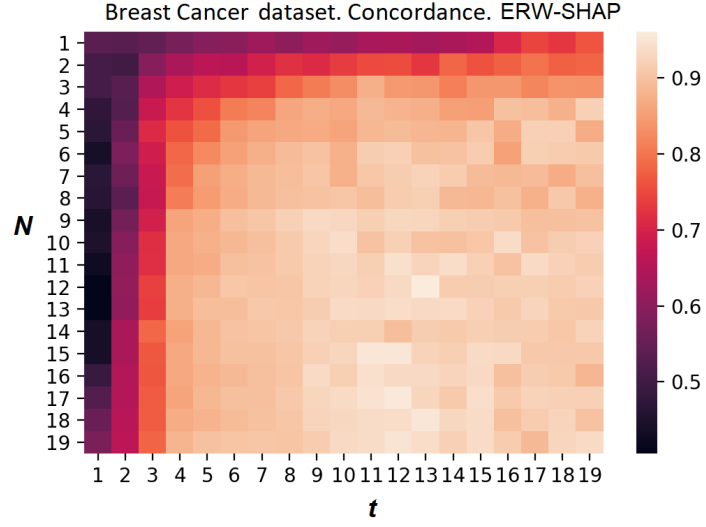


Figure 24: The heatmap reflecting the concordance index C obtained by ERW-SHAP for the Breast Cancer dataset

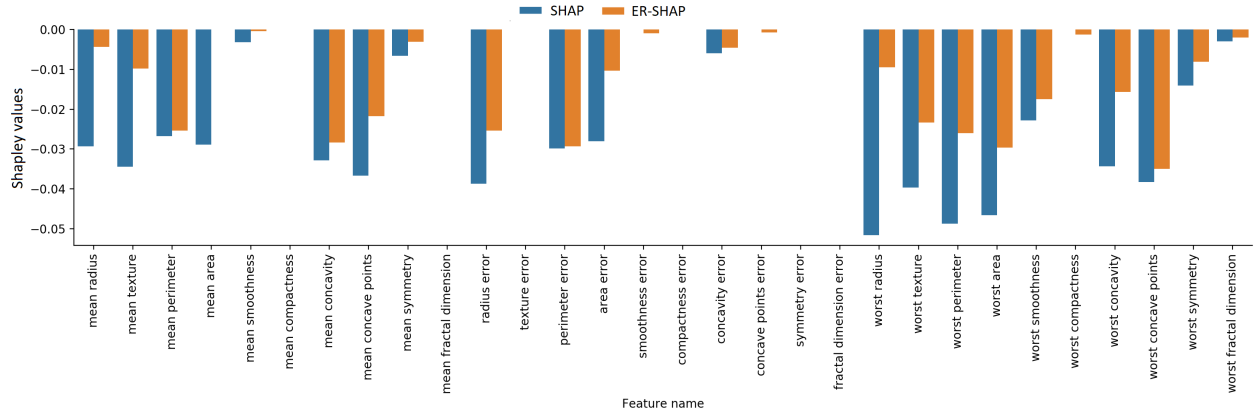


Figure 25: Shapley values obtained by means of SHAP and ER-SHAP as functions of N for the Breast Cancer dataset

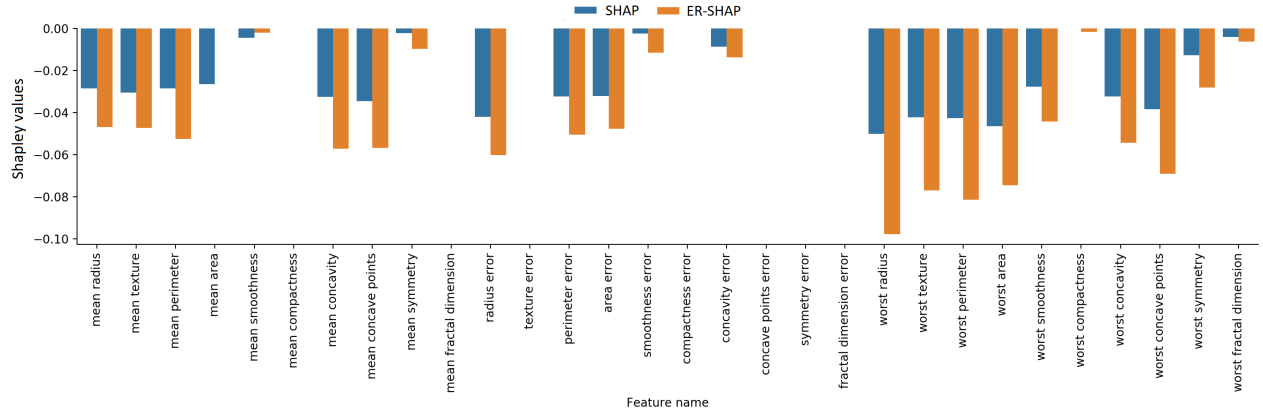


Figure 26: Shapley values obtained by means of SHAP and ERW-SHAP as functions of N for the Breast Cancer dataset under condition of using the normal distribution of feature changes with the standard deviation 0.1

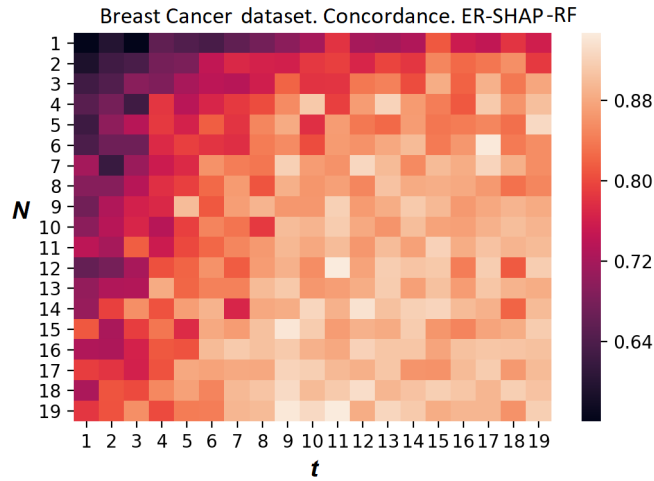


Figure 27: The heatmap reflecting the concordance index C obtained by ER-SHAP-RF for the Breast Cancer dataset without using the temperature scaling

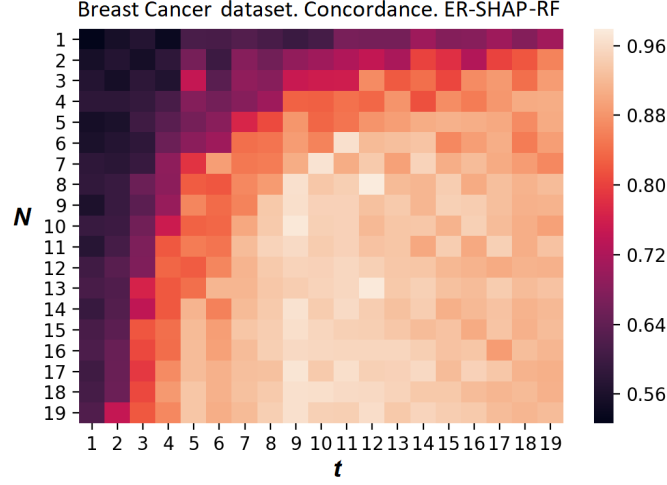


Figure 28: The heatmap reflecting the concordance index C obtained by ER-SHAP-RF for the Breast Cancer dataset with using the temperature scaling

6 Conclusion

It is important to note that only three modifications of the ensemble-based SHAP have been presented. At the same time, many additional modifications of the general approach based on constructing the ensemble of SHAPs can be developed following the proposed modifications and the idea of the ensemble-based approximation.

First of all, the model of the feature selection used in ER-SHAP-RF for “pre-training” can be changed. There are many methods solving the feature selection problem. Moreover, simple explanation methods can be also applied to the preliminary selection of important features and to computing their probability distribution.

Second, various rules different from averaging can be applied to combining the results of SHAPs, for example, the largest (smallest) Shapley values can be computed for providing pessimistic (optimistic) decisions.

The ensemble-based approach can be applied to explanation of the classification as well as regression black-box models. It gives many opportunities for developing new methods which can be viewed as directions for further research. The proposed approach can be applied to local and global explanations. However, its main advantage is that it significantly reduces the computation time for solving the explanation problem.

Acknowledgement

The research is partially funded by the Ministry of Science and Higher Education of the Russian Federation as part of World-class Research Center program: Advanced Digital Technologies (contract No. 075-15-2020-934 dated 17.11.2020).

References

- [1] K. Aas, M. Jullum, and A. Løland. Explaining individual predictions when features are dependent: More accurate approximations to Shapley values. *arXiv:1903.10464*, Mar 2019.
- [2] A. Adadi and M. Berrada. Peeking inside the black-box: A survey on explainable artificial intelligence (XAI). *IEEE Access*, 6:52138–52160, 2018.
- [3] R. Agarwal, N. Frosst, X. Zhang, R. Caruana, and G.E. Hinton. Neural additive models: Interpretable machine learning with neural nets. *arXiv:2004.13912*, April 2020.
- [4] M. Ancona, C. Oztireli, and M. Gros. Explaining deep neural networks with a polynomial time algorithm for Shapley values approximation. *arXiv:1903.10992*, Mar 2019.
- [5] L. Antwarg, R.M. Miller, B. Shapira, and L. Rokach. Explaining anomalies detected by autoencoders using SHAP. *arXiv:1903.02407v2*, June 2020.
- [6] A.B. Arrieta, N. Diaz-Rodriguez, J. Del Ser, A. Bennetot, S. Tabik, A. Barbado, S. Garcia, S. Gil-Lopez, D. Molina, R. Benjamins, R. Chatila, and F. Herrera. Explainable artificial intelligence (XAI): Concepts, taxonomies, opportunities and challenges toward responsible AI. *arXiv:1910.10045*, October 2019.
- [7] V. Belle and I. Papantonis. Principles and practice of explainable machine learning. *arXiv:2009.11698*, September 2020.
- [8] J. Bento, P. Saleiro, A.F. Cruz, M.A.T. Figueiredo, and P. Bizarro. TimeSHAP: Explaining recurrent models through sequence perturbations. *arXiv:2012.00073*, November 2020.
- [9] Y. Bi, D. Xiang, Zongyuan Ge, F. Li, C. Jia, and J. Song. An interpretable prediction model for identifying N7-methylguanosine sites based on XGBoost and SHAP. *Molecular Therapy: Nucleic Acids*, 22:362–372, 2020.
- [10] L. Bouneder, Y. Leo, and A. Lachapelle. X-SHAP: towards multiplicative explainability of machine learning. *arXiv:2006.04574*, June 2020.
- [11] D. Bowen and L. Ungar. Generalized SHAP: Generating multiple types of explanations in machine learning. *arXiv:2006.07155v2*, June 2020.
- [12] L. Breiman. Random forests. *Machine learning*, 45(1):5–32, 2001.
- [13] D.V. Carvalho, E.M. Pereira, and J.S. Cardoso. Machine learning interpretability: A survey on methods and metrics. *Electronics*, 8(832):1–34, 2019.
- [14] C.-H. Chang, S. Tan, B. Lengerich, A. Goldenberg, and R. Caruana. How interpretable and trustworthy are gams? *arXiv:2006.06466*, June 2020.
- [15] G. Chuan, G. Pleiss, Y. Sun, and K.Q. Weinberger. On calibration of modern neural networks. In *International Conference on Machine Learning*, volume PMLR, pages 1321–1330, 2017.

- [16] I.C. Covert, S. Lundberg, and S.-I. Lee. Explaining by removing: A unified framework for model explanation. *arXiv:2011.14878*, November 2020.
- [17] A. Das and P. Rad. Opportunities and challenges in explainable artificial intelligence (XAI): A survey. *arXiv:2006.11371v2*, June 2020.
- [18] G.V. den Broeck, A. Lykov, M. Schleich, and D. Suci. On the tractability of SHAP explanations. *arXiv:2009.08634v2*, January 2021.
- [19] C. Frye, D. de Mijolla, L. Cowton, M. Stanley, and I. Feige. Shapley-based explainability on the data manifold. *arXiv:2006.01272*, June 2020.
- [20] D. Garreau and D. Mardaoui. What does LIME really see in images? *arXiv:2102.06307*, February 2021.
- [21] D. Garreau and U. von Luxburg. Explaining the explainer: A first theoretical analysis of LIME. *arXiv:2001.03447*, January 2020.
- [22] D. Garreau and U. von Luxburg. Looking deeper into tabular LIME. *arXiv:2008.11092*, August 2020.
- [23] R. Guidotti, A. Monreale, S. Ruggieri, F. Turini, F. Giannotti, and D. Pedreschi. A survey of methods for explaining black box models. *ACM computing surveys*, 51(5):93, 2019.
- [24] T. Hastie and R. Tibshirani. *Generalized additive models*, volume 43. CRC press, 1990.
- [25] T.K. Ho. The random subspace method for constructing decision forests. *IEEE transactions on pattern analysis and machine intelligence*, 20(8):832–844, 1998.
- [26] Q. Huang, M. Yamada, Y. Tian, D. Singh, D. Yin, and Y. Chang. GraphLIME: Local interpretable model explanations for graph neural networks. *arXiv:2001.06216*, January 2020.
- [27] A. Jung. Explainable empirical risk minimization. *arXiv:2009.01492*, September 2020.
- [28] A.V. Konstantinov and L.V. Utkin. Interpretable machine learning with an ensemble of gradient boosting machines. *arXiv:2010.07388*, October 2020.
- [29] M.S. Kovalev, L.V. Utkin, and E.M. Kasimov. SurvLIME: A method for explaining machine learning survival models. *Knowledge-Based Systems*, 203:106164, 2020.
- [30] I.E. Kumar, S. Venkatasubramanian, C. Scheidegger, and S. Friedler. Problems with shapley-value-based explanations as feature importance measures. In *International Conference on Machine Learning*, pages 5491–5500. PMLR, 2020.
- [31] Y. Liang, S. Li, C. Yan, M. Li, and C. Jiang. Explaining the black-box model: A survey of local interpretation methods for deep neural networks. *Neurocomputing*, 419:168–182, 2021.
- [32] Y. Lou, R. Caruana, and J. Gehrke. Intelligible models for classification and regression. In *Proceedings of the 18th ACM SIGKDD International Conference on Knowledge Discovery and Data Mining*, pages 150–158. ACM, August 2012.

- [33] S.M. Lundberg and S.-I. Lee. A unified approach to interpreting model predictions. In *Advances in Neural Information Processing Systems*, pages 4765–4774, 2017.
- [34] S. Mangalathu, S.-H. Hwang, and J.-S. Jeon. Failure mode and effects analysis of RC members based on machinelearning-based SHapley Additive exPlanations (SHAP) approach. *Engineering Structures*, 219:110927 (1–10), 2020.
- [35] R. Marcinkevics and J.E. Vogt. Interpretability and explainability: A machine learning zoo mini-tour. arXiv:2012.01805, December 2020.
- [36] C. Molnar. *Interpretable Machine Learning: A Guide for Making Black Box Models Explainable*. Published online, <https://christophm.github.io/interpretable-ml-book/>, 2019.
- [37] H. Nori, S. Jenkins, P. Koch, and R. Caruana. InterpretML: A unified framework for machine learning interpretability. arXiv:1909.09223, September 2019.
- [38] V. Petsiuk, A. Das, and K. Saenko. RISE: Randomized input sampling for explanation of black-box models. arXiv:1806.07421, June 2018.
- [39] J. Rabold, H. Deininger, M. Siebers, and U. Schmid. Enriching visual with verbal explanations for relational concepts: Combining LIME with Aleph. arXiv:1910.01837v1, October 2019.
- [40] A. Redelmeier, M. Jullum, and K. Aas. Explaining predictive models with mixed features using shapley values and conditional inference trees. In *Machine Learning and Knowledge Extraction. CD-MAKE 2020*, volume 12279 of *Lecture Notes in Computer Science*, pages 117–137, Cham, 2020. Springer.
- [41] M.T. Ribeiro, S. Singh, and C. Guestrin. “Why should I trust You?” Explaining the predictions of any classifier. arXiv:1602.04938v3, Aug 2016.
- [42] M.T. Ribeiro, S. Singh, and C. Guestrin. Anchors: High-precision model-agnostic explanations. In *AAAI Conference on Artificial Intelligence*, pages 1527–1535, 2018.
- [43] R. Rodriguez-Perez and J. Bajorath. Interpretation of machine learning models using shapley values: application to compound potency and multi-target activity predictions. *Journal of Computer-Aided Molecular Design*, 34:1013–1026, 2020.
- [44] B. Rozemberczki and R. Sarkar. The shapley value of classifiers in ensemble games. arXiv:2101.02153, January 2021.
- [45] C. Rudin. Stop explaining black box machine learning models for high stakes decisions and use interpretable models instead. *Nature Machine Intelligence*, 1:206–215, 2019.
- [46] O. Sagi and L. Rokach. Explainable decision forest: Transforming a decision forest into an interpretable tree. *Information Fusion*, 61:124–138, 2020.
- [47] S.M. Shankaranarayana and D. Runje. ALIME: Autoencoder based approach for local interpretability. arXiv:1909.02437, Sep 2019.

- [48] L.S. Shapley. A value for n-person games. In *Contributions to the Theory of Games*, volume II of *Annals of Mathematics Studies* 28, pages 307–317. Princeton University Press, Princeton, 1953.
- [49] J.L. Speiser, M.E. Miller, J. Tooze, and E. Ip. A comparison of random forest variable selection methods for classification prediction modeling. *Expert Systems With Applications*, 134:93–101, 2019.
- [50] E. Strumbelj and I. Kononenko. An efficient explanation of individual classifications using game theory. *Journal of Machine Learning Research*, 11:1–18, 2010.
- [51] E. Strumbelj and I. Kononenko. A general method for visualizing and explaining black-box regression models. In *Adaptive and Natural Computing Algorithms. ICANNGA 2011*, volume 6594 of *Lecture Notes in Computer Science*, pages 21–30, Berlin, 2011. Springer.
- [52] E. Strumbelj and I. Kononenko. Explaining prediction models and individual predictions with feature contributions. *Knowledge and Information Systems*, 41:647–665, 2014.
- [53] N. Takeishi. Shapley values of reconstruction errors of PCA for explaining anomaly detection. arXiv:1909.03495, September 2019.
- [54] N. Xie, G. Ras, M. van Gerven, and D. Doran. Explainable deep learning: A field guide for the uninitiated. arXiv:2004.14545, April 2020.
- [55] J. Yu, Z. Lin, J. Yang, X. Shen, X. Lu, and T.S. Huang. Generative image inpainting with contextual attention. In *Proceedings of the IEEE Conference on Computer Vision and Pattern Recognition*, pages 5505–5514, 2018.
- [56] H. Yuan, H. Yu, J. Wang, K. Li, and S. Ji. On explainability of graph neural networks via subgraph explorations. arXiv:2102.05152, February 2020.
- [57] E. Zablocki, H. Ben-Younes, P. Perez, and M. Cord. Explainability of vision-based autonomous driving systems: Review and challenges. arXiv:2101.05307, January 2021.
- [58] M.D. Zeiler and R. Fergus. Visualizing and understanding convolutional networks. In *ECCV 2014*, volume 8689 of *LNCS*, pages 818–833, Cham, 2014. Springer.
- [59] X. Zhang, S. Tan, P. Koch, Y. Lou, U. Chajewska, and R. Caruana. Axiomatic interpretability for multiclass additive models. In *In Proceedings of the 25th ACM SIGKDD International Conference on Knowledge Discovery & Data Mining*, pages 226–234. ACM, 2019.
- [60] Y. Zhang, P. Tino, A. Leonardis, and K. Tang. A survey on neural network interpretability. arXiv:2012.14261, December 2020.